STRAIGHT LINES IN LINEAR ARRAY SCANNER IMAGERY

Ayman Habib, Devin Kelley, Andinet Asmamaw
Department of Civil and Environmental Engineering and Geodetic Science
The Ohio State University
habib.1@osu.edu, kelley.83@osu.edu, asmamaw.1@osu.edu

ISPRS Commission III

KEY WORDS: Linear Features, Linear Array Scanners, Aerial Triangulation

ABSTRACT

Increased use of digital imagery has facilitated the opportunity to use features, in addition to points, in photogrammetric applications. Straight lines are often present in object space, and prior research has focused on incorporating straight-line constraints into the bundle adjustment for frame imagery. In this research, we introduce a straight-line constraint in the bundle adjustment for linear array scanners. A linear array scanner scene is acquired using different geometry than frame cameras. A scene is composed of a sequence of images, each of which may be slightly shifted against each other due to slight changes in the system's trajectory. As a result, straight lines in object space do not appear as straight lines in image space. The proposed bundle adjustment constraint accommodates this distortion. The underlying principal in this constraint is that the vector from the perspective center to a scene point on a straight-line feature lies on the plane defined by the perspective center and the two object points defining the straight line. This constraint utilizes the perspective transformation model for point features in linear array scanner imagery. The proposed technique makes use of straight-line features in object space, and aids in the recovery of the exterior orientation parameters as well as adding to the geometric strength of the bundle adjustment. This constraint has been embedded in a bundle adjustment software application, developed at the Ohio State University, that models frame and linear array scanner imagery

1. INTRODUCTION

Most photogrammetric applications are based on the use of distinct points. These points are often obtained through measurements in an analog or digital environment. Recently, more attention has been drawn to linear features. There are several motivations for the utilization of linear features in photogrammetry:

- Points are not as useful as linear features when it comes to higher level tasks such as object recognition.
- Automation of the map making process is one of the major tasks in digital photogrammetry and cartography. It is easier to automatically extract linear features from the imagery rather than distinct points (Kubik, 1988).
- Images of a man made environment are rich with linear features.

Habib (1999) discusses the various options for straight-line representation in photogrammetric applications. The primary representation considerations are uniqueness and singularities. In this research, straight lines in object space are represented by using two points along the line. In this way, the line segment is well localized in the object space. This representation is attractive because such coordinates can be easily introduced or obtained from a GIS database.

Previous research on linear features in photogrammetry has focused primarily on frame imagery. Straight-line constraints can be incorporated into the bundle adjustment by utilizing the fact that the perspective transformation of a straight line is also a straight line. Mikhail and Weerawong (1994) proposed a straight-line constraint that constrains a unit vector defining the object space line, the vector from the perspective center to a point on the object line, and the vector from the perspective center to the image point to be coplanar. In their approach, the object line is represented as an infinite line segment. Habib (1999) proposed a straight-line constraint, which forces the plane defined by the image line to be coplanar with the plane defined by the perspective center and two object points defining the line. In this approach the object line is defined by two points, localizing it in space. These techniques rely on the use of frame imagery.

computer, a clock generator, and a disk array unit with a capacity of 256 GB for data recording. The movement and position of the aircraft is measured and stored by a flight control system containing a DGPS system and an Inertial Navigation System (INS). Additional information about the AeS-1 System is reported by Schwäbisch and Moreira (1999).

Operating Frequency	9.35 – 9.75 GHz
Wavelength	3.12 – 3.25 cm
Polarization	HH
PRF	1.5 kHZ – 16 kHz
Peak Power	1.9 kW
Ground Resolution	up to 0.5 m x 0.5 m
Radiometric Resolution	up to 1.8 db
Swath Width	1 – 15 km
Flight Velocity	50 – 200 m/s
Typical Flight Altitude	500 – 9000 m
InSAR Baseline	0.5 or 1.8 m
Dimensions	W: 1.2 m, H: 1.0 m, D: 0.6 m
Weight	210 kg including antennas
Power	28 V, 60 A maximum

Table 1: System parameters of AeS-1 flight segment

Figure 1: Gulfstream Commander 1000 with AeS-1 X-band antenna boom construction

3 DATA PROCESSING AND VALIDATION

The processing of the digitally stored "latent" SAR raw data to visible images can be divided into three processing steps. First the raw data stored on hard disks are transcribed and backuped on Digital Linear Tapes (DLTs). In SAR processing the raw data are read from the DLT, decoded and correlated by using a Range/Doppler algorithm. The positional acurracy is improved by including the motion compensation data, generated itselves of the DGPS and INS data. Single-look images in complex format are the SAR processor output. Multi-look processing eliminates the harmful influence of the Speckle on image radiometry at the cost of lowered ground resolution. Hence, a trade-off between speckled appearance and resolution must be found. In figure 2 for example a 37 look image with ground resolution of 2.5 meters was generated from the initial 0.2 meters single look image. In a further step an interferometric processor coregistrates the images of the two antennas for producing an interferogram and a DEM in slant-range geometry. Also a magnitude of the complex correlation coefficient and the SAR magnitude is carried out. In a last step the geometry of the ready processed data must be changed from slant-range to a georectified cartographic reference system. This is done using marked and measured reference points, so called Corner Reflectors (CR) (see white spot in the center of figure 2). To obtain images of a predefined area, e.g. of a map sheet, the single tracks must be mosaicked and trimmed. To suppress artifacts in the data, e.g. caused by Radar shadows, data sets flown in opposite directions also can be combined.

Before deriving information from the SAR data, the positional and height accuracy must be verified. This was made with a data set from a well-known testsite near Solothurn, Switzerland, located on the border of the Swiss Jura mountains and the tertiary basin. The site contains different kinds of surface structures e.g. plains, hills, and open areas, as well as forests, rivers and build-up areas in a small space.

The positional accuracy was checked by superimposing the SAR amplitude image with a large scaling topographic map (1 : 10,000) (Fig. 2). The deviations between the map and the image are less than three meters. For validating the height acurracy of the InSAR-DEM it was compared with 24 trigonometric fixed points of the Federal Office of Topography Wabern, Switzerland. The average difference was 13.7 cm with standard deviation of 17.3 cm (Meier 1999). This accuracies allow the production of topographic maps in scales ranging from 1 : 10,000 to 1 : 50,000 and smaller. The highest resolution is occasionally necessary for map derivation. For small scaled maps a lower resolution is sufficient, which leads to a faster processing and a cheaper production.
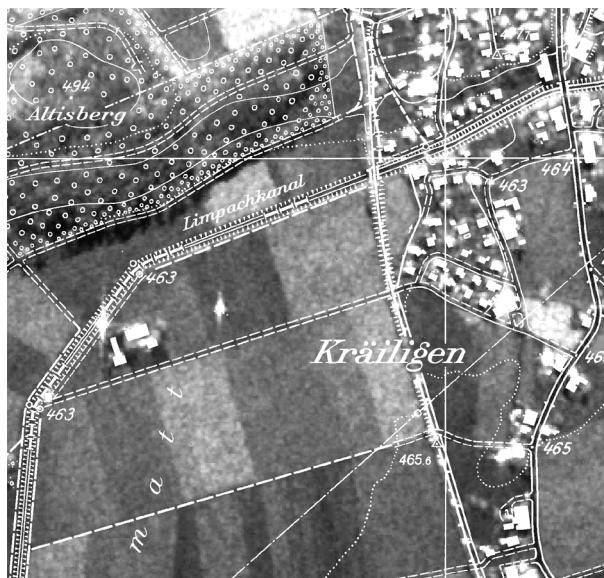
Figure 2: Terrain-geocoded SAR scene of an area
near Solothurn with superimposed topographic map
(scale 1 : 10,000)
(© Vermessungsamt d. Kantons Bern, Switzerland)

4   MAP GENERATION

For the map production as described in this paper, two information extraction methods are applied: visual interpretation and a supervised classification.

To accerelate and simplify map production the first step after basic data preparation is to investigate the maximum number of distinguishable classes. This was realized by programming a classification software optimized for the high resolution SAR data. The used input data for the software are fully geocod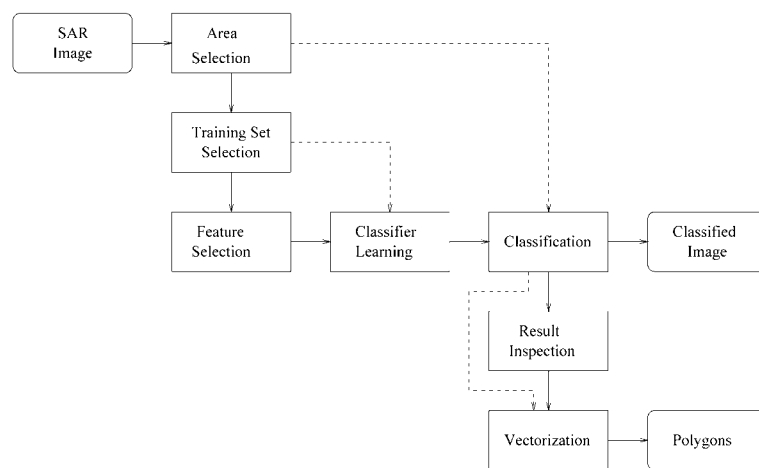ed SAR images and DEMs. Typical classes of interest in topographic mapping are water, forest, build-up and open areas. After the user had choosen training examples inside the graphical user interface (GUI) for the classes of interest an artificial neutral network (ANN) classifier is designed. The used ANN classifier is the well-known Multilayer Perceptrom (MLP) (Rumelhart *et al.* 1986). An interactive component allows inspection of intermediate results and enables feedback to training set selection and classifier learning, thus an online learning capability is established (Fig. 3). The borders of the classes of the improved final results are vectorized, stored in individual layers and outputted in DXF format. This vector data can be integrated e.g. in a DTP program or cartographic information system (CIS) and combined with the data achieved by manual screen digitizing.

Figure 3: Block diagram of the ANN classifier

In a further step of the InSAR processing chain the third dimension of the terrain, represented by contour lines and hill-shading, must be produced and embedded into the map. To automatize the extraction of the contour lines from the existing geocoded InSAR DEM (see chapter 3), a software system was developed by Schmieder and Huber (2000). Due to the fact, that microwaves with short wavelength' (e.g. X-band) cannot penetrate into buildings and dense vegetation like forests, the contour lines represent only the surface of that areas which lead to an error in height. With complex algorithms its possible to extract that areas and correct the DEM there (Huber/Schmieder 1997). The output product is

labelled, generalized employing the Douglas-Peuker algorithm and finally converted to contour-lines in DXF format. The 3-dimensional nature of the terrain can be visualized by simple hill-shading, which was rendered automatically from the same DEM.

Visual SAR image interpretation needs lots of experience and knowledge about the SAR imaging principles and geometry, because they obey other regularities than optical sensors. Before each interpretation an interpretation key has to be elaborated and controlled. In this key all the derivable objects in the data are described. Also in times where analysis of remote sensing images by digital methods increases, the visual information extraction using human interpretation ability is still significant. Till this day the visual image interpretation is the most accurate method of information extraction. On the other hand the method is very cost expensive and time-consuming. For this investigation classification was mainly applied for forests, open areas and large rivers and lakes. Objects like build-up areas, road networks, single buildings and other cartographic signatures had to be interpreted and digitized by the operator. In some cases it is difficult to distinguish small rivers from roads. Therefore the information provided by contour-lines are very helpful and instructive. After extracting the interpreted map objects by screen digitizing in a simplified vector graphic (Fig. 5.2), the layout graphic is transformed into the final map graphic (Fig. 5.3).

All the additional information, not extractable from remote sensing data but important for understanding maps, like map scripting must be taken from other sources e.g. Internet, other maps, or on site. Figure 4.1 to 4.3 show the steps from the SAR data to be interpreted, the three classified classes and the final map completed with visually interpreted objects. The generated data are combined in a professional WYSIWYG graphic software and prepared for printing.

5 MAP SAMPLES

After processing the InSAR data, described in chapter 3, the following map extracts were generated by visual image interpretation (Fig. 5) or by a combination of classification and visual interpretation (Fig. 4).
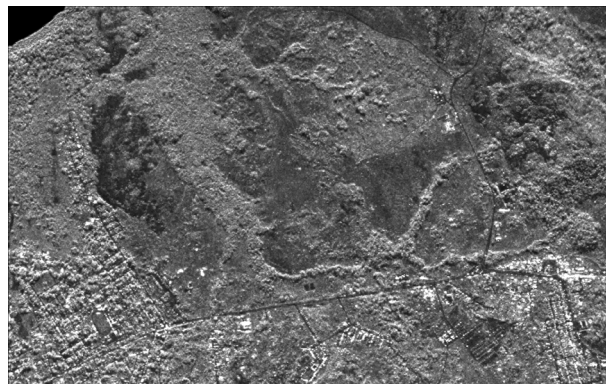

Figure 4.1: Geocoded SAR ortho image,
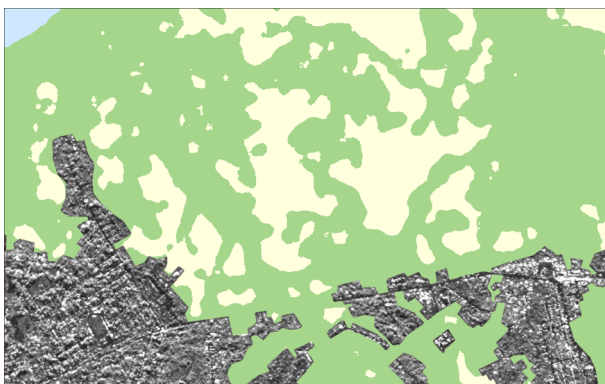4.0 km by 2.5 km, scale 1: 50,000

Figure 4.2: Classification result: Forest...green
(medium grey), open area...yellow (light grey)
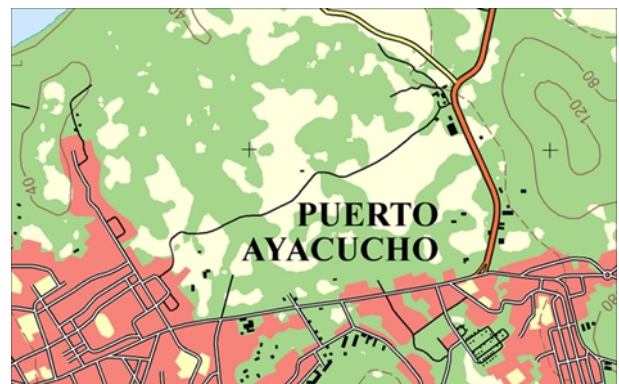and water...blue (upper left corner)

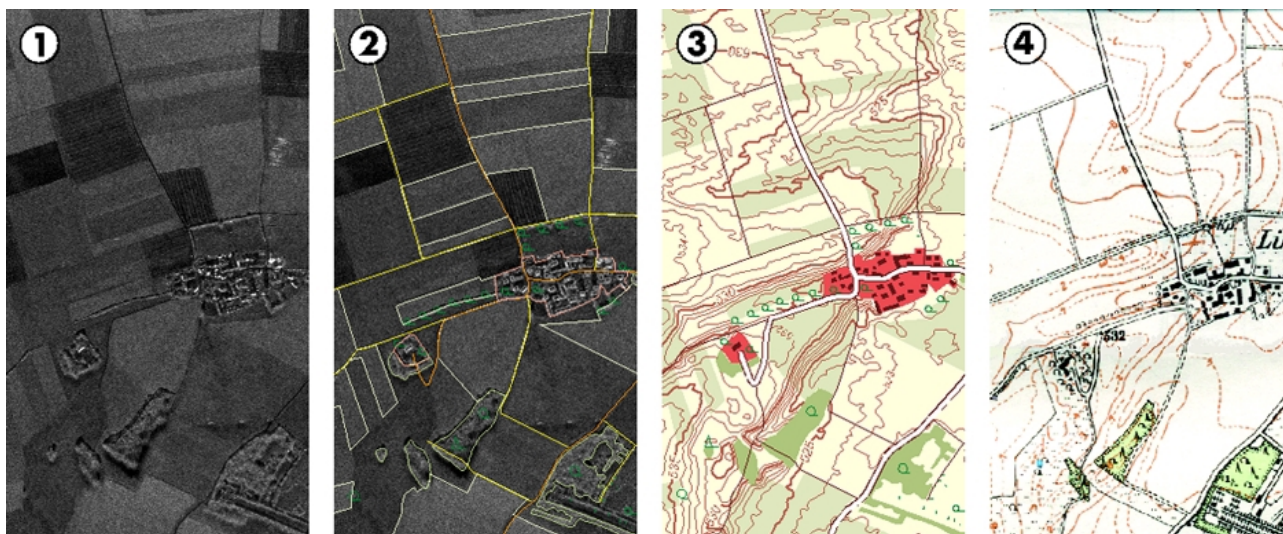Figure 4.3: Topographic map, scale 1 : 50,000

Figure 5: Derivation of a topographic map 1 : 25,000 by visual image interpretation:
(1) AeS-1 X-band ortho image, (2) digitized map layout, (3) topographic map in final map design,
(4) official topographic map for comparison (© Bayerisches Landesvermessungsamt München, Germany)

6   CONCLUSIONS

In this paper an operational approach using high-resolution InSAR data for the production of topographic maps was presented. These type of maps can be produced for countries where only old maps or maps in a small scale are available. Future investigations tend to integrate the derived data into a Cartographic and/or Geographic Information System (CIS/GIS) or using the data for updating of existing databases (Keim 1997). The accuracy of the contour lines in forested areas could be improved by using a SAR-sensor employing longer wavelength (e.g. P-band) (Hofmann *et al.* 1999). The classification results can be improved by assisting the classifier with the information of SAR coherence. To summarize, the shown method supplies maps with a high amount of cartographic and topographic information, produced on a high level of automation and in a cost-efficient way.

REFERENCES

Huber R. and Schmieder A., 1997. Automatic Extraction of Cartographic Features from Airborne Interferometric SAR data, Proceeding of EUROPTO Symposium on Aerospace Remote Sensing, London, UK, Great Britain, pp. 188-196.

Hofmann C., Schwäbisch M., Och S., Wimmer C.,Moreira J., 1999. Multipath P-Band Interferometry – First Results, Proceeding of the 4th International Airborne Remote Sensing Conference & Exhibition, Ottawa, Canada, pp. II-732-737.

Keim A., 1997. Untersuchung zur Fortführung von ATKIS®-DLM 25-Daten durch visuelle Interpretation von SAR-Bildern, Diploma thesis, Polytechnic University Munich, Germany.

Meier E., 1999. Validierung der AeS-InSAR-Oberflächenmodelle, Internal validation letter, Remote Sensing Laboratories (RSL) University Zürich-Irchel, Switzerland.

Rumelhart D., Hinton G., Williams R., 1986. Learning Internal Representations by Error Propagation in Parallel and Distributed Processing: Explorations in the Microstructure of Cognition. Vol. I, Foundations MIT Press, Cambridge, MA, U.S.A., pp. 318-362.

Schmieder A. and Huber R., 2000. Automatic Generation of Contour Lines for Topographic Maps by Means of Airborne High-Resolution Interferometric Radar Data, Proceeding of the ASPRS Annual Conference Proceedings, Washington, DC, U.S.A.

Schwäbisch M. and Moreira J., 1999. The High Resolution Airborne Interferometric SAR AeS-1, Proceeding of the 4th International Airborne Remote Sensing Conference and Exhibition, Ottawa, Canada, pp. I-540-547.